



Formation mechanism and source apportionment of water-soluble organic carbon in PM₁, PM_{2.5} and PM₁₀ in Beijing during haze episodes

5 Qing Yu^{1,2}, Jing Chen^{1,2}, Weihua Qin^{1,2}, Yuepeng Zhang^{1,2}, Siming Cheng^{1,2}, Mushtaq Ahmad^{1,2},
Xingang Liu^{1,2}, Hezhong Tian^{1,2}

¹State Key Joint Laboratory of Environment Simulation and Pollution Control, School of Environment, Beijing Normal University, Beijing 100875, China.

²Center of Atmospheric Environmental Studies, Beijing Normal University, Beijing 100875, China.

Correspondence to: Jing Chen (jingchen@bnu.edu.cn)

10 **Abstract.** Water soluble organic carbon (WSOC) in atmospheric aerosols may pose significant impacts on haze formation,
climate change, and human health. This study investigated the distribution characteristics and sources of WSOC in Beijing
based on the diurnal PM₁, PM_{2.5} and PM₁₀ samples collected during haze episodes in winter and early spring of 2017. The
haze episode in winter showed elevated level of WSOC, around three times of that in spring. WSOC was enriched in PM_{2.5}
in winter while the proportions in both finer (0-1 μm) and coarse particles (2.5-10 μm) increased in spring. Several organic
15 tracers were carefully selected and measured to demonstrate the sources and formation mechanism of WSOC. Most of the
identified organic tracers showed similar seasonal variation, diurnal change and size distributions with WSOC, while the
biogenic secondary organic aerosol (SOA) tracer *cis*-pinonic acid was an obvious exception. Based on the distribution
characteristics of the secondary organic tracers and their correlation patterns with key influencing factors, the importance of
the gas-phase versus aqueous-phase oxidation processes on SOA formation was explored. The gas-phase photochemical
20 oxidation was weakened during haze episodes, whereas the aqueous-phase oxidation became the major pathway of SOA
formation, especially in winter, at night and for the coarser particles. Secondary sources accounted for more than 50% of
WSOC in both winter and spring. Biomass burning was not the dominant source of WSOC in Beijing during haze episodes.
Primary sources showed greater influence on finer particles while secondary sources became more important for coarser
particles during haze episode in winter. SOC estimated by the OC-EC method, WSOC-levoglucosan method, and PMF-
25 based methods were comparable, and the potential errors for different SOC estimation methods were discussed.



1 Introduction

Organic aerosols constitute a significant fraction (20-60 % by mass) of atmospheric particulate matter, in which water-soluble organic carbon (WSOC) accounts for 20-80 % of total organic carbon (Jaffrezo et al., 2005; Du et al., 2014; Tang et al., 2016). WSOC can alter the hygroscopicity of atmospheric aerosols, thus affecting aerosol size distribution and their ability to act as cloud condensation nuclei (CCN) (Ervens et al., 2011). Besides, WSOC may pose significant risk to human health as it is closely associated with the formation of reactive oxygen species (ROS) and cytotoxicity of atmospheric aerosols (Velali et al., 2016; Bae et al., 2017).

Due to the high proportion of WSOC in atmospheric aerosols and their environmental impact, the sources of WSOC have been widely discussed in the literature with a general recognition that WSOC mainly originates from direct emissions of biomass burning and secondary formation through the oxidation of volatile organic compounds in the atmosphere (Ding et al., 2008b; Feng et al., 2013; Du et al., 2014). Nevertheless, previous studies have also shown that primary emission sources other than biomass burning, such as vehicular exhaust emission, residual oil combustion, etc., also contribute to the WSOC load in the atmosphere (Kawamura and Kaplan, 1987; Guo et al., 2015; Kuang et al., 2015). Such primary emissions may even surpass biomass burning and become the major sources of WSOC (Kaul et al., 2014). Compared to the primary sources, estimate of the contributions of secondary components has been difficult when studying the sources of WSOC. For example, the chemical mass balance (CMB) model, a typical receptor model frequently used in aerosol source apportionment, can not quantify the specific contribution of each secondary source due to the lack of source profiles (Zheng et al., 2006; Ding et al., 2008a). The tracer-yield method based on the chamber experiments usually ignores the cloud process and the subsequent aqueous-phase reactions, thus may bring about large uncertainties when applying the secondary organic aerosol (SOA) yield results obtained under simple chamber conditions to the actual atmosphere (Kleindienst et al., 2007; Feng et al., 2013). In contrast, the positive matrix factorization (PMF) model combined with organic tracers has proved to be effective in quantifying the contributions of different secondary as well as primary sources of WSOC. For example, Feng et al. (2013) reported the sources and seasonal variations of WSOC and SOA in Shanghai based on PMF model and several SOA tracers.

The concentration, composition and sources of WSOC in atmospheric aerosols show significant regional and seasonal variations in China and worldwide (Jaffrezo et al., 2005; Ervens et al., 2011; Feng et al., 2013; Du et al., 2014; Kuang et al., 2015). As SOA takes a large proportion of WSOC, the sources of WSOC are in fact greatly impacted by meteorological conditions (Kaul et al., 2014). North China, particularly the Beijing-Tianjin-Hebei region, has been subject to frequent regional haze episodes in recent years. Research on haze formation and evolution showed that the highly polluted haze episodes were usually associated with high relative humidity and increased water-soluble fraction of $PM_{2.5}$ (Chen et al., 2014; Tian et al., 2014; Cheng et al., 2015). As water-soluble ions and the formation of secondary inorganic aerosols in haze episodes have been extensively studied, few studies focused on the water-soluble organic compounds and SOA formation. In fact, the formation of SOA during haze episodes can be influenced by the elevated levels of anthropogenic pollutants such as sulfate and NO_x (Hoyle et al., 2011; Xu et al., 2015). Therefore, identifying the contributions of primary sources and



60 secondary formation to WSOC during haze episodes would help to elucidate the complex nature of WSOC and further put forward the effective control measures.

In this study, diurnal PM_{10} , $PM_{2.5}$ and PM_{10} samples were collected at an urban site of Beijing during haze episodes in January, March, and April, 2017. The carbonaceous (OC, EC, WSOC) contents, water-soluble ions and typical organic tracers in each sample were measured. The contributions of primary versus secondary sources to WSOC during the sampling
65 periods were identified using PMF. The objectives of this study were to (1) clarify the distribution characteristics of WSOC in PM_{10} , $PM_{2.5}$ and PM_{10} during haze episodes, (2) quantify the contributions of primary and secondary sources to WSOC in PM_{10} , $PM_{2.5}$ and PM_{10} , (3) and elucidate the formation mechanism of secondary components in WSOC during haze episodes. In addition, estimates of SOC via different methods were also compared and evaluated.

2 Experimental

70 2.1 Field sampling

The sampling site was located on the roof of the School of Environment Building (about 20 m above ground) in Beijing Normal University, representing a typical urban environment. Diurnal PM_{10} , $PM_{2.5}$ and PM_{10} samples were collected in winter and early spring of 2017, including the winter period of Dec. 31, 2016-Jan. 10, 2017, and the spring periods of Mar. 15-Mar 25, 2017 and Apr. 3-Apr. 7, 2017, covering haze episodes during the sampling periods. The PM_{10} , $PM_{2.5}$ and PM_{10}
75 samples were simultaneously collected on pre-baked (500 °C for 4 h) quartz filters (PALLFLEX, 90 mm) using three independent medium-volume air samplers (Qingdao Hengyuan Technology Development Co., Ltd., HY-100) at a flow rate of 100 L min⁻¹. The daytime samples were collected from 8:00 to 19:30 and the nighttime samples from 20:00 to 7:30 the next day. After being stabilized under constant temperature (25 °C) and humidity (50 %), the filters were precisely weighed using an analytical balance (Sartorius, BSA124S, reading precision 0.1 mg) before and after sampling. The sample filters
80 were sealed in polyethylene bags and stored below -20 °C in a refrigerator for further analysis. In total, 63 and 90 samples were collected for the haze episodes in winter and spring respectively.

2.2 Chemical analysis

Seven organic tracers were measured for each sample, including levoglucosan, cholesterol, 4-methyl-5-nitrocatechol, phthalic acid, 2-methylerythritol, 3-hydroxyglutaric acid, and *cis*-pinonic acid. One-fourth of each sample filter was cut into
85 pieces and ultrasonically extracted with 10 mL methanol for 20 min for three times. The combined extracts were filtrated through a 0.45 µm PTFE syringe filter, concentrated using a rotary evaporator, and then blown to dryness under a gentle stream of ultrapure nitrogen. A mixture of 100 µL pyridine and 200 µL N,O-bis-(trimethylsilyl) trifluoroacetamide (BSTFA, with 1 % trimethylchlorosilane as catalyst) was added to react at 75 °C for 70 min. The derivatives were then diluted with n-hexane to 1 mL and immediately analyzed by a Shimadzu TQ8040 gas chromatography-mass spectrometry (GC-MS) in



90 electron ionization (EI) mode. A RXi-5SiIMS capillary column (30 m × 0.25 mm i.d., film thickness 0.25 μm) was used as the GC column and helium was used as the carrier gas (1.0 mL min⁻¹). The injector was set splitless at an temperature of 290 °C. The programmed oven temperature increased from 70 °C to 150 °C at 2 °C min⁻¹, then to 200 °C at 5 °C min⁻¹, then to 300 °C at 25 °C min⁻¹, and stay at 300 °C for 6 min. The organic tracers were quantified using the calibration curves of the derivatives of authentic standards, which were obtained right before the measurement of the ambient samples.

95 The recovery rates of the measured organic tracers were determined by measuring the authentic standards spiked onto the pre-baked blank quartz filters following the same procedure as the ambient samples. The recovery rates of the measured organic tracers were in the range of 70-110 %, except for 4-methyl-5-nitrocatechol, which showed recoveries of 36-57 % with an average of 47.8 %. The relative standard deviation (RSD) of the measurement of 4-methyl-5-nitrocatechol was 18.0 % based on four repeated measurements, which met the analysis requirement of environmental samples (RSD < 30 %).
100 Therefore, the concentration of 4-methyl-5-nitrocatechol was corrected for recovery, while that of other organic tracers was not. The blank filters found no significant contamination (< 10 % of the concentration in ambient samples), and the final ambient concentrations were corrected for blank.

To measure the contents of water-soluble organic carbon (WSOC) and water-soluble inorganic ions, one-fourth of each sample filter was cut into pieces and ultrasonically extracted with 35 mL Milli-Q water (> 18.2 MΩ) for 40 min. The extract
105 was filtered through a 0.45 μm PTFE syringe filter and split into two portions. One portion was used to quantify WSOC by a total organic carbon (TOC) analyzer (Shimadzu TOC-L CPN), and the other was used to measure the four anions (Cl⁻, NO₃⁻, SO₄²⁻, C₂O₄²⁻) and five cations (Na⁺, NH₄⁺, K⁺, Mg²⁺, Ca²⁺) by a Dionex 600 ion chromatography. In addition, the concentrations of organic carbon (OC) and elemental carbon (EC) were analyzed by a DRI 2001A carbon analyzer following the IMPROVE thermal/optical reflectance (TOR) protocol.

110 2.3 Source apportionment by PMF

EPA PMF 5.0 was used to quantify the contributions of primary and secondary sources to WSOC as well as OC in aerosols of different sizes. A total of 16 species were chosen as the inputs of PMF, including WSOC, OC, EC, SO₄²⁻, NO₃⁻, NH₄⁺, C₂O₄²⁻, Ca²⁺, Mg²⁺, levoglucosan, cholesterol, 4-methyl-5-nitrocatechol, phthalic acid, 2-methylerythritol, 3-hydroxyglutaric acid, and *cis*-pinonic acid. The concentration uncertainties of the target species were calculated as follow:

$$115 \quad Unc = 5/6 \times MDL \quad (c \leq MDL) \quad (1)$$

$$Unc = \sqrt{(P \times c)^2 + (0.5 \times MDL)^2} \quad (c > MDL) \quad (2)$$

where MDL is the minimum detection limit of the measuring instrument, P is the measurement error fraction, and c is the concentration of target species. The measurement error fraction was set to 10 % by experience for WSOC, OC, EC, SO₄²⁻, NO₃⁻, NH₄⁺, C₂O₄²⁻, Ca²⁺, and Mg²⁺ (Gao et al., 2014; Yang et al., 2016b). The error fractions of organic tracers were
120 estimated by the relative standard deviation of repeated tests: the values for levoglucosan, cholesterol, 2-methylerythritol, 3-hydroxyglutaric acid and phthalic acid were set to 10 %, and the values of 4-methyl-5-nitrocatechol and *cis*-pinonic acid



were set to 15 %. The PMF model was run repeatedly with minor adjustment of factor numbers and uncertainties to get the optimal solution.

2.4 Aerosol water content calculation and other supplementary data collection

- 125 To explore the formation mechanism of secondary organic tracers, the inorganic aerosol water content (AWC) in PM_{10} , $PM_{2.5}$ and PM_{10} was estimated by the reverse mode calculation of ISORROPIA-II model, which is a computationally efficient thermodynamic equilibrium model for inorganic aerosols (Fountoukis and Nenes, 2007). The contribution of organic compounds to AWC was estimated by the same approach employed by Cheng et al. (2016). The total AWC was the sum of the water content in inorganic and organic aerosols.
- 130 The hourly concentration data of $PM_{2.5}$, PM_{10} , O_3 , and NO_2 that were measured at an urban air quality monitoring station (39.89° N, 116.38° E) were obtained online (<http://www.envicloud.cn>). The meteorological data including temperature (T), relative humidity (RH), wind speed (WS), wind direction (WD), solar radiation (SR) and precipitation were recorded at the sampling site using an automatic meteorological station. The average temperature, relative humidity, and wind speed was 2.1° C, 64.2 %, and 0.85 m s^{-1} , respectively for the winter period, and 12.5° C, 64.9 % and 0.89 m s^{-1} for the spring periods.
- 135 One precipitation process occurred from the night of March 22nd to the night of March 24th during the whole sampling period, and the total rainfall was 13.4 mm.

3 Results and discussion

3.1 Distribution characteristics of WSOC in PM_{10} , $PM_{2.5}$ and PM_{10} during haze episodes

- The temporal variations of WSOC, OC and particulate mass concentrations in PM_{10} , $PM_{2.5}$ and PM_{10} in Beijing during the whole sampling period are shown in Fig. 1 and the average concentrations of the identified species in PM_{10} , $PM_{2.5}$ and PM_{10}
- 140 during haze episodes with $PM_{2.5}$ higher than $75\text{ }\mu\text{g m}^{-3}$ are provided in Table 1. Compared to the haze episodes in spring, the haze episode in winter was characterized by higher particulate mass concentrations and more stagnant weather conditions as indicated by lower wind speed, lower temperature, and higher relative humidity. Compared to the total particulate matter, the mass concentrations of WSOC and OC in the corresponding particulate matter showed stronger seasonal variations, and the
- 145 average mass concentrations of WSOC and OC during the haze episode in winter were around three times of those in spring (Table 1). Both WSOC and OC were enriched in $PM_{2.5}$ during the haze episode in winter with comparable mass concentrations in the size ranges of $0\text{-}1\text{ }\mu\text{m}$ and $1\text{-}2.5\text{ }\mu\text{m}$, while the proportions in both finer ($0\text{-}1\text{ }\mu\text{m}$) and coarse particles ($2.5\text{-}10\text{ }\mu\text{m}$) increased in spring.

- As secondary organic aerosol takes a large proportion of WSOC, the WSOC/OC ratio can be used to infer the extent of
- 150 secondary formation and/or aging of aerosols (Ram et al., 2012). As shown in Fig. 1, the WSOC/OC ratio remained relatively stable during polluted days and the ratio sharply dropped when wind or rain cleansed the atmosphere of particulate



matter. Compared to the WSOC/OC ratios reported in the literature (Table S1), the average WSOC/OC ratio during the haze episodes in this study are significantly higher than the corresponding seasonal averages in Beijing, which was probably attributable to the enhanced SOA production during haze days (Cheng et al., 2013a; Zhou et al., 2014). The severe SOA pollution during the haze episodes was also evidenced by the high OC/EC ratios as shown in Table 1. The WSOC/OC ratio in spring was obviously higher than that in winter, indicating higher proportion of secondary or more aged aerosols in spring. Similar seasonal variation of WSOC/OC was also reported in the literature (Table S1), which was probably due to the enhanced production of secondary aerosols at higher temperature (Jaffrezo et al., 2005; Xiang et al., 2017). As also shown in Table 1, the WSOC/OC ratio was higher during the day than that at night, which was consistent with the stronger photochemical processes and enhanced secondary formation during the day. The WSOC/OC ratios in PM₁, PM_{2.5} and PM₁₀ were very similar during the haze episode in winter, while the ratios in PM₁, PM_{2.5} and PM₁₀ showed greater difference in spring with the general order of PM₁ > PM_{2.5} > PM₁₀.

3.2 Distribution and chemical characteristics of organic tracers

3.2.1 Mass concentrations of organic tracers during haze episodes

The average mass concentrations of the identified organic tracers in PM₁, PM_{2.5} and PM₁₀ during haze episodes with PM_{2.5} higher than 75 µg m⁻³ are also shown in Table 1. The identified organic tracers covered three major source categories of WSOC, including primary sources, anthropogenic SOA and biogenic SOA. Levoglucosan and cholesterol are primary WSOC tracers for biomass burning and cooking, respectively. Phthalic acid and 4-methyl-5-nitrocatechol are anthropogenic SOA tracers for aromatic SOA and biomass burning SOA, respectively (Iinuma et al., 2010; Al-Naiema and Stone, 2017). 2-methylerythritol, 3-hydroxyglutaric acid and *cis*-pinonic acid are biogenic SOA tracers with 2-methylerythritol acting as isoprene SOA tracer and 3-hydroxyglutaric acid and *cis*-pinonic acid as monoterpene SOA tracers. Compared to the reported values of organic tracers in the literature, the average mass concentrations of primary WSOC tracers and anthropogenic SOA tracers (levoglucosan, cholesterol and phthalic acid) in PM_{2.5} during the haze episodes were 0.7-13.2 times higher than the corresponding seasonal averages in Beijing (He et al., 2006; Tao et al., 2016; Zhao et al., 2018), while the average mass concentrations of biogenic SOA tracers (2-methylerythritol, 3-hydroxyglutaric acid, *cis*-pinonic acid) in PM_{2.5} during the haze episodes in winter and spring were 0.4-6.2 times lower than those in summer in urban Beijing (Yang et al., 2016a).

As shown in Table 1, both the primary WSOC tracers and the anthropogenic SOA tracers in PM₁, PM_{2.5} and PM₁₀ showed elevated mass concentrations during the haze episode in winter compared to those in spring. In addition, the average mass concentrations of the anthropogenic SOA tracers (phthalic acid and 4-methyl-5-nitrocatechol) in winter were around 5 times of those in spring while the average mass concentrations of the primary WSOC tracers (levoglucosan and cholesterol) in winter were around 2.5 times of those in spring, showing enhanced SOA formation from anthropogenic precursors during the haze episode in winter. Both the low atmospheric mixing height during the haze episode in winter and the additional emissions of anthropogenic precursors (such as polycyclic aromatic hydrocarbons) associated with domestic heating resulted



185 in the accumulation of anthropogenic precursors and consequently the anthropogenic SOA. On the contrary, the average
mass concentrations of monoterpene SOA tracers (*cis*-pinonic acid and 3-hydroxyglutaric acid) in spring were higher than
those in winter, which probably resulted from the enhanced biogenic monoterpene emissions and SOA formation at higher
temperature (Cheng et al., 2018). However, different from the monoterpene SOA tracers, the isoprene SOA tracer, 2-
methylerythritol, showed higher concentration in winter. Previous studies reported emissions of large amounts of isoprene
from all biomass burning types (Akagi et al., 2011; Li et al., 2018). Therefore, the intense biomass burning activities in
190 winter as evidenced by the high concentration of levoglucosan may contribute to the enhanced concentration of isoprene as
well as its SOA tracer in winter. In addition, previous studies also showed that sulfate could increase the solubility of
isoprene-derived epoxydiols (IEPOX) in the aqueous phase of aerosols through salting-in effect, and promote the ring-
opening reaction of IEPOX and the subsequent isoprene SOA formation through nucleophilic attack (Xu et al., 2015; Li et
al., 2018). Therefore, the higher concentration of 2-methylerythritol during the haze episode in winter may also be
195 attributable to the enhanced SOA formation from isoprene in the presence of higher concentration of sulfate as shown in
Table 1.

3.2.2 Diurnal patterns and size distributions

The diurnal patterns of the organic tracers in PM₁, PM_{2.5} and PM₁₀ during the haze episodes (PM_{2.5} > 75 μg m⁻³) in winter
and spring are shown in Fig. 2. Compared to the nighttime, the daytime atmosphere is typically characterized by higher
200 atmospheric mixing height and stronger source emissions & atmospheric photochemical activities, which exert opposite
effects on the diurnal patterns of atmospheric pollutants. For example, the WSOC concentration was slightly higher at night
than that by day in winter whereas the diurnal pattern of WSOC was opposite in spring (Table 1), which was probably due to
the different dominating atmospheric processes in winter and spring. As shown in Fig. 2 and Table 1, the concentrations of
the primary WSOC tracers and anthropogenic SOA tracers were much higher at night in winter, whereas the daytime and
205 nighttime concentrations were similar in spring due to the smaller diurnal difference of atmospheric mixing height and
stronger daytime photochemical activities in spring compared to winter. However, levoglucosan (primary biomass burning
tracer) in aerosols of all sizes and 4-methyl-5-nitrocatechol (SOA tracer from biomass burning) in PM_{2.5} and PM₁₀ were
exceptions, which showed significantly higher concentrations at night in spring. It was speculated that the greatly enhanced
nighttime concentrations of levoglucosan and 4-methyl-5-nitrocatechol in spring resulted from the uncontrolled burning
210 activities of biomass at night. Similar phenomenon has also been reported in our previous study (Yang et al., 2016b). The
monoterpene SOA tracer *cis*-pinonic acid showed higher concentrations in the daytime in both seasons with greater diurnal
variation in spring compared to winter, indicating the dominant effect of photochemical oxidation and secondary formation
by day. In contrast, another monoterpene SOA tracer 3-hydroxyglutaric acid showed similar daytime and nighttime
concentrations in both seasons and the isoprene SOA tracer 2-methylerythritol showed higher concentration at night
215 especially in spring. Compared to *cis*-pinonic acid, 2-methylerythritol and 3-hydroxyglutaric acid are higher-generation
oxidation products of biogenic precursors and are formed in longer time scales (Fu et al., 2010). As such, the direct



220 promoting effect of photochemical activities during the daytime was weaker on them than that on *cis*-pinonic acid. Besides, the enhanced 2-methylerythritol at night in spring was probably due to the enhanced emission of isoprene from biomass burning, which was consistent with the diurnal patterns of levoglucosan and 4-methyl-5-nitrocatechol in spring. Except for *cis*-pinonic acid and 3-hydroxyglutaric acid, the identified organic tracers showed the least diurnal difference in PM₁ compared to PM_{2.5} and PM₁₀.

225 Most of the identified organic tracers showed similar size distributions with WSOC with enrichment in PM_{2.5} and comparable mass concentrations in the size ranges of 0-1 μm and 1-2.5 μm during the haze episode in winter and increased proportions in finer (0-1 μm) or coarse particles (2.5-10 μm) in spring (Fig. 2 and Table 1). *Cis*-pinonic acid was an exception and was mainly distributed in PM₁ during all the haze episodes in winter and spring, consistent with the previously reported results (Kavouras and Stephanou, 2002; Herckes et al., 2006). The enrichment of *cis*-pinonic acid in PM₁ indicates that *cis*-pinonic acid in atmospheric aerosols was formed through gas-phase photochemical reactions and nucleation, which results in the accumulation in finer particles (Yu et al., 1999). As for other SOA tracers including 4-methyl-5-nitrocatechol, phthalic acid, 2-methylerythritol, and 3-hydroxyglutaric acid, a considerable fraction of them were distributed in the size range of 1-10 μm especially 1-2.5 μm, which possibly resulted from the hygroscopic growth of aerosols and the facilitated aqueous-phase oxidation on the surface of particles during haze episodes. Besides, the proportions of these SOA tracers in the size range of 1-10 μm were higher at night than by day, and higher in winter than in spring, implying higher contributions of aerosol hygroscopic growth and aqueous-phase oxidation to the formation and distribution of these SOA tracers at night and in winter.

235 3.2.3 Influencing factors and possible formation mechanisms of SOA tracers

To explore the influencing factors of SOA tracers, the correlation coefficients between SOA tracers and several meteorological parameters, O₃, aerosol acidity [H⁺], and aerosol water content (AWC) in PM₁, PM_{2.5} and PM₁₀ during the whole sampling period are listed in Table 2. The comparison of the correlation coefficients among different SOA tracers in PM_{2.5} is shown in Fig. 3. Overall, the anthropogenic SOA tracers 4-methyl-5-nitrocatechol and phthalic acid exhibited relatively strong positive correlations with aerosol water content, aerosol acidity and relative humidity and relatively strong negative correlations with wind speed, temperature, solar radiation and O₃. Typically, higher wind speed, higher temperature, and lower relative humidity are associated with higher atmospheric mixing height, thereby are favorable for the dispersion of atmospheric pollutants (Zhang et al., 2017). Besides, the strong negative correlations of the anthropogenic SOA tracers with O₃ and solar radiation as well as temperature suggest that gas-phase photo-oxidation was not the major formation mechanism for 4-methyl-5-nitrocatechol and phthalic acid during the haze episodes. Instead, the secondary formation was enhanced by aqueous-phase oxidation and aerosol acidity during the haze episodes as evidenced by the strong positive correlations with aerosol water content, aerosol acidity and relative humidity. Chamber studies also showed that increasing particle water content could significantly enhance the aromatic SOA yield (Zhou et al., 2011).



Compared to the anthropogenic SOA tracers, the monoterpene SOA tracer *cis*-pinonic acid showed distinctively different correlations with the factors under consideration. Overall, *cis*-pinonic acid showed strong positive correlation with temperature, moderate positive correlation with solar radiation, O₃ and aerosol acidity, and poor correlation with aerosol water content, relative humidity and wind speed. Previous studies also showed that higher temperature could enhance monoterpene emission and the subsequent SOA formation (Ding et al., 2011; Shen et al., 2015). Consistent with the formation mechanism inferred from the diurnal pattern and size distribution of *cis*-pinonic acid (Sec. 3.2.2), the correlation pattern of *cis*-pinonic acid with different influencing factors further proved that the gas-phase photochemical oxidation was the major formation pathway of *cis*-pinonic acid. As shown in Fig. 3, compared with *cis*-pinonic acid, aerosol water content and relative humidity became more important factors influencing the concentrations of 3-hydroxyglutaric acid and 2-methylerythritol while their correlations with temperature, solar radiation, and O₃ became weaker or even negative. Therefore, it was inferred that the formation of 3-hydroxyglutaric acid and 2-methylerythritol was a combination of the gas-phase and aqueous-phase oxidation processes with 3-hydroxyglutaric acid more on the gas-phase oxidation side and 2-methylerythritol more on the aqueous-phase oxidation side.

The formation mechanism of 2-methylerythritol from isoprene has been extensively studied in the literature. Basically, the production of 2-methylerythritol from isoprene can be achieved through two pathways, including the gas-phase oxidation with OH radical and the acid-catalyzed multiphase reactions with hydrogen peroxide (Claeys et al., 2004a; Claeys et al., 2004b). The formation of 2-methylerythritol can be enhanced by the reactive uptake and subsequent aqueous-phase oxidation of the isoprene-derived epoxydiols (IEPOX) formed in the gas phase (Surratt et al., 2010; Xu et al., 2015; Riva et al., 2016). Previous study showed that the concentration of 2-methyltetrols increased with temperature rapidly on days with temperature higher than 20 °C (Liang et al., 2012). However, the temperature range covered in this study was relatively low with the average of 2.1 °C in winter and 12.5 °C in spring. Therefore, the enhancement of the gas-phase oxidation at higher temperature in spring was probably masked by other factors such as the decreased rate of aqueous-phase oxidation and reduced emissions from biomass burning.

The correlation pattern of WSOC/OC with different influencing factors was similar with that of 3-hydroxyglutaric acid, and relative humidity and aerosol water content appeared to be crucial factors affecting the WSOC/OC ratio (Table 2). The strong positive correlations with RH and aerosol water content were attributable to two facts: (1) the gas-phase WSOC could more easily partition into the aerosol phase at higher aerosol water content (Hennigan et al., 2009); (2) the aqueous-phase production of WSOC could be enhanced at higher aerosol water content (Du et al., 2014; Xiang et al., 2017). The correlation patterns of the SOA tracers with different influencing factors show slight difference among PM₁, PM_{2.5} and PM₁₀. One general rule that can be reached was that the correlation coefficients of 4-methyl-5-nitrocatechol, phthalic acid, 2-methylerythritol, and 3-hydroxyglutaric acid with relative humidity and aerosol water content increased with particle size, indicating higher contributions of the aqueous oxidation process to the formation of these compounds in larger aerosols following the hygroscopic growth of aerosols during haze episodes.



3.3 Source apportionment of WSOC in PM₁, PM_{2.5} and PM₁₀ during haze episodes

3.3.1 Source apportionment by PMF

The primary and secondary sources of WSOC were quantified by the PMF 5.0 model with WSOC, EC, SO₄²⁻, NO₃⁻, NH₄⁺,
285 C₂O₄²⁻, Ca²⁺, Mg²⁺, and the seven organic tracers as the inputs of PMF. Theoretically, the source profiles of WSOC would be
different in different seasons and for particles with different sizes. However, considering the sample size requirement by
PMF (preferably more than 100 samples), we assumed that the source profile of WSOC was identical in different seasons
and for particles with different sizes and used the whole-period concentration data as one input into the PMF model to obtain
the source profile of WSOC. Such simplification was justified as the inputs of the source profile were carefully selected
290 representative source tracers.

As shown in Fig. 4, nine factors for the source apportionment of WSOC were identified in this study, including four primary
sources and five secondary sources. Factors 1 and 2 were characterized by a high level of levoglucosan and cholesterol
respectively, thus were identified as primary emissions from biomass burning and cooking respectively. Factor 3 showed a
high loading of EC that could not be interpreted by biomass burning, indicating emissions from other primary combustion
295 sources such as coal combustion. High levels of Ca²⁺, Mg²⁺ were observed in Factor 4, which was thus interpreted as dust
source. Factors 5 and 6 were characterized by a high level of 4-methyl-5-nitrocatechol and phthalic acid respectively, thus
were identified as secondary organic carbon (SOC) from biomass burning and aromatic compounds respectively. Factor 7
showed a high loading of 2-methylerythritol, and was identified as SOC from isoprene. Factor 8 showed high levels of *cis*-
pinonic acid and 3-hydroxyglutaric acid, and was identified as SOC from monoterpenes. Factor 9 exhibited a strong link
300 with SO₄²⁻, NO₃⁻, NH₄⁺ and C₂O₄²⁻, suggesting a secondary nature of this factor, thus was interpreted as SOC from other
sources.

Source contributions to WSOC in PM₁, PM_{2.5} and PM₁₀ in Beijing during the sampling periods in winter and spring are
presented in Fig. 5. The contributions of secondary sources to WSOC were more than 50 % in both winter and spring. The
major sources of WSOC in winter were other primary combustion sources and aromatic SOC, and their contributions
305 decreased significantly in spring when the contributions of other SOC and biogenic SOC obviously increased. Domestic
heating was probably the major cause of the enhancement of other primary combustion sources and aromatic SOC in winter.
According to the results of previous studies, biomass burning contributed to more than 30 % of WSOC in PM_{2.5} in winter
and was therefore the dominant source of wintertime WSOC in Beijing (Cheng et al., 2013b; Du et al., 2014; Tao et al.,
2016). In contrast, the contribution of biomass burning (Factor 1 + Factor 5) to WSOC in PM_{2.5} in the current study was
310 22.1 % and 17.9 % in winter and spring respectively, much lower than the previously reported results. The decreased
contribution of biomass burning was possibly due to the effective control of biomass burning around Beijing in recent years,
or it might also indicate the enhanced contributions of other sources during haze episodes compared to the non-haze days.
Moreover, the contribution of biomass burning to WSOC was more in the form of secondary formation rather than primary



emission in winter while primary emission became the dominant form in spring, indicating different burning pattern and
315 secondary reaction mechanism in winter and spring. Cooking and dust contributed the least to WSOC, while their
contributions were both increased in spring compared to winter.

Comparing the source contributions of WSOC in PM₁, PM_{2.5} and PM₁₀, it can be found that the contribution of the sum of
primary sources to WSOC followed the order of PM₁ > PM_{2.5} > PM₁₀ in winter, implying that primary sources have greater
influence on finer particles. Higher correlation between WSOC and POC (primary organic carbon) in PM₁ than that in PM_{2.5}
320 was also observed during haze episodes in Shanghai (Qiao et al., 2016). The increased contribution of secondary sources in
coarser particles during haze episode in winter was likely associated with the hygroscopic growth of aerosols and the
enhanced secondary formation through aqueous phase oxidation. The contributions of the total primary and secondary
sources to WSOC in spring were around 40 % and 60 % respectively. While the primary and secondary contributions were
similar in PM₁, PM_{2.5} and PM₁₀ in spring, the contributions of the respective sources were different. In particular, the
325 contribution of other primary combustion sources to WSOC decreased in larger particles in spring while that of biomass
burning obviously increased.

3.3.2 Comparison of SOC estimated using different methods

Quantifying SOA in the atmosphere has been difficult and several methods have been used to roughly estimate the amounts
of SOA, including the OC-EC method, WSOC-levoglucosan method, and PMF-based methods. To evaluate the potential
error of different SOC estimation methods, SOC estimated by different methods were compared. The estimation of SOC by
330 the OC-EC method was calculated by $SOC_{OC-EC} = OC - (OC/EC)_{min} \times EC$, where $(OC/EC)_{min}$ is the minimum OC to EC ratio
during the sampling period, representing the OC to EC ratio from primary emissions (Lim and Turpin, 2002). The minimum
OC to EC ratios in PM₁, PM_{2.5} and PM₁₀ during the whole sampling period were 1.84, 2.08, 2.03, respectively, which
appeared on the non-haze night of January 8th, 2017 with strong wind and low relative humidity. The WSOC-levoglucosan
335 method is based on the assumption that SOC is water-soluble and WSOC mainly derives from biomass burning and SOC.
Thus SOC was estimated by $SOC_{WSOC-Levo} = WSOC - (WSOC/Levo)_{BB} \times C_{Levo}$, where $(WSOC/Levo)_{BB}$ is the ratio of WSOC
to levoglucosan from biomass burning, and C_{Levo} is the ambient concentration of levoglucosan (Ding et al., 2008b). The ratio
of 10 was used as the $(WSOC/Levo)_{BB}$ ratio in winter as suggested by Yan et al. (2015), whereas the ratio of 8 was used in
spring as suggested by Feng et al. (2013). In fact, the $(WSOC/Levo)_{BB}$ ratio would change with the types of biomass and the
340 burning conditions, thus could vary significantly in different locations and seasons. Besides, the $(WSOC/Levo)_{BB}$ ratio might
also be different in aerosols of different sizes. Hence, the rough estimation of $(WSOC/Levo)_{BB}$ would result in considerable
uncertainty in the estimation of SOC. Moreover, it is questionable that all SOC is soluble in water. In fact, large contribution
of water-insoluble secondary organic aerosols has been observed in urban environment, which was attributed to the reactions
of anthropogenic precursors (Favez et al., 2008; Sciare et al., 2011).



345 The PMF-based methods included the WSOC-PMF and OC-PMF methods with WSOC and OC as the total variable in the
model respectively. The five secondary sources of WSOC/OC resolved by PMF were summed up to calculate SOC:
SOC_{WSOC/OC-PMF} = isoprene SOC + monoterpene SOC + aromatic SOC + biomass burning SOC + other SOC. Source
apportionment of OC by PMF was performed in the same way as WSOC, and the results are shown in Figures S1 and S2.
Comparing the source contributions of WSOC and OC, it was found that primary sources particularly other primary
350 combustion sources and dust contributed more to OC than to WSOC.

Fig. 6 and Table 3 show the comparison of secondary organic carbon in PM₁, PM_{2.5} and PM₁₀ in Beijing estimated by
different methods during the sampling periods in winter and spring, and Table S2 shows the correlation coefficients among
the estimated SOCs. Generally, SOC estimated by different methods exhibited similar trends during the whole sampling
period, and the correlations were particularly strong ($R > 0.89$) in winter. In spring, however, the OC-EC method showed
355 poorer correlation with other methods, especially the PMF-based methods ($0.40 < R < 0.79$). The two PMF-based methods
showed the highest correlation with each other ($R > 0.95$). Overall, the estimated SOC from the OC-based methods (OC-EC
and OC-PMF methods) were higher than that from the WSOC-based methods (WSOC-levoglucosan and WSOC-PMF
methods) especially in winter, indicating substantial contribution of water-insoluble SOC to total SOC in the atmosphere.
Therefore, the SOC value estimated from the WSOC-based methods at best described the secondary portion of water-soluble
360 carbon in the atmosphere; using such value to represent total SOC in the atmosphere would result in underestimation of SOC
in the atmosphere. Comparatively, SOC_{WSOC-Levo} was obviously higher than SOC_{WSOC-PMF}, probably due to the overlook of
the contributions of other primary combustion sources by the WSOC-levoglucosan method and thus SOC_{WSOC-Levo} was
overestimated.

The OC-EC method is frequently used in the literature to estimate secondary organic aerosol concentration in the atmosphere
365 for its convenience. As shown in Fig. 6 and Table 3, SOC_{OC-EC} was close to SOC_{OC-PMF} in winter, while in spring, SOC_{EC} was
significantly lower than SOC_{OC-PMF} in PM_{2.5} and PM₁₀. Noting that SOC_{OC-EC} did not meet the decreasing trend of PM₁₀ >
PM_{2.5} > PM₁ during some days and that the OC-EC method showed poorer correlations with other methods, we suspected
that non-negligible errors existed in the measurement of OC/EC. It has been reported that the OC and EC values would be
significantly different using different analytical methods, especially for the EC value (Cheng et al. 2011a). For example,
370 compared to the thermal-optical transmittance (TOT) method, the thermal-optical reflectance (TOR) method would obtain
higher EC values and lower OC values, thus the estimated SOC values would be lower if the TOR method was used to
measure OC and EC (Cheng et al. 2011; Xiang et al., 2017). Though the OC data was also used in the SOC estimation by
PMF methods, SOC_{OC-PMF} was estimated by based on SOA tracers rather than EC values, thus was less affected by the
OC/EC measurement methods.



375 4 Conclusions

Based on the diurnal PM₁, PM_{2.5} and PM₁₀ samples collected in Beijing during haze episodes in winter and early spring, WSOC, OC, EC, water-soluble ions and organic tracers were accurately measured to investigate the distribution characteristics and sources of WSOC. The values of WSOC, OC and WSOC/OC ratio were all much higher during the haze episodes in this study compared to the seasonal averages in Beijing, suggesting higher pollution level of organic compounds and enhanced secondary formation during the haze episodes. Due to the additional contribution from domestic heating and the more stagnant weather conditions in winter, the haze episode in winter showed elevated levels of WSOC and OC, around three times of those in spring. Both WSOC and OC were enriched in PM_{2.5} during the haze episode in winter with comparable mass concentrations in the size ranges of 0-1 μm and 1-2.5 μm, while the proportions in both finer (0-1 μm) and coarse particles (2.5-10 μm) increased in spring.

385 Most of the identified organic tracers showed similar seasonal variation, diurnal change and size distributions with WSOC, with elevated concentrations and more significant diurnal difference in winter and enrichment in PM_{2.5}. The biogenic SOA tracer cis-pinonic acid was an obvious exception, which showed higher concentration in spring, higher concentration during the day, and major distribution in PM₁. Based on the distribution characteristics and correlation patterns with the influencing factors, it was inferred that cis-pinonic acid was mainly formed through the gas-phase photochemical oxidation while other SOA tracers were closely associated with the aqueous-phase oxidation. The gas-phase photochemical oxidation was weakened during the haze episodes, whereas the aqueous-phase oxidation became the major pathway of SOA formation during the haze episodes, especially in winter, at night and for the coarser particles.

395 Secondary sources accounted for more than 50% of WSOC in both winter and spring. The major sources of WSOC in winter were other primary combustion sources and aromatic SOC, whereas the contributions of other SOC and biogenic SOC obviously increased in spring. Contrary to the existing research results, biomass burning was not the dominant source of WSOC in Beijing during haze episodes. Moreover, the contribution of biomass burning to WSOC was more in the form of secondary formation in winter while primary emission became the dominant form in spring, indicating different burning pattern and secondary reaction mechanism in winter and spring. Primary sources showed greater influence on finer particles during haze episode in winter; however, secondary sources became more important for coarser particles, possibly due to the enhanced secondary formation through aqueous phase oxidation following the hygroscopic growth of aerosols.

400 SOC estimated by the OC-EC method, WSOC-levoglucosan method, and PMF-based methods were comparable during the whole sampling period, and the following points need to be taken into account when estimating SOC. (1) Water-insoluble SOC should not be ignored. (2) The WSOC-levoglucosan method may overestimate the secondary portion of WSOC due to overlook of other primary combustion sources. (3) SOC estimated by the OC-EC method may be underestimated when the TOR method was used to measure OC and EC. (4) SOC estimated by the PMF model was less affected by the measuring



methods of OC and EC, and increasing the number of samples and SOA tracers would improve the accuracy of SOC estimation.

References

- Akagi, S. K., Yokelson, R. J., Wiedinmyer, C., Alvarado, M. J., Reid, J. S., Karl, T., Crounse, J. D., and Wennberg, P. O.:
410 Emission factors for open and domestic biomass burning for use in atmospheric models, *Atmos. Chem. Phys.*, 11, 4039-4072,
doi:10.5194/acp-11-4039-2011, 2011.
- Al-Naiema, I. M. and Stone, E. A.: Evaluation of anthropogenic secondary organic aerosol tracers from aromatic
hydrocarbons, *Atmos. Chem. Phys.*, 17, 2053-2065, doi:10.5194/acp-17-2053-2017, 2017.
- Bae, M. S., Schauer, J. J., Lee, T., Jeong, J. H., Kim, Y. K., Ro, C. U., Song, S. K., and Shon, Z. H.: Relationship between
415 reactive oxygen species and water-soluble organic compounds: Time-resolved benzene carboxylic acids measurement in the
coastal area during the KORUS-AQ campaign, *Environ. Pollut.*, 231, 1-12, doi:10.1016/j.envpol.2017.07.100, 2017.
- Chen, J., Qiu, S. S., Shang, J., Wilfrid, O. M. F., Liu, X. G., Tian, H. Z., and Boman, J.: Impact of Relative Humidity and
Water Soluble Constituents of PM_{2.5} on Visibility Impairment in Beijing, China, *Aerosol Air Qual. Res.*, 14, 260-268,
doi:10.4209/aaqr.2012.12.0360, 2014.
- 420 Cheng, C. L., Wang, G. H., Zhou, B. H., Meng, J. J., Li, J. J., Cao, J. J., and Xiao, S.: Comparison of dicarboxylic acids and
related compounds in aerosol samples collected in Xi'an, China during haze and clean periods, *Atmos. Environ.*, 81, 443-449,
doi:10.1016/j.atmosenv.2013.09.013, 2013a.
- Cheng, X., Li, H., Zhang, Y. J., Li, Y. P., Zhang, W. Q., Wang, X. Z., Bi, F., Zhang, H., Gao, J., Chai, F. H., Lun, X. X.,
Chen, Y. Z., Gao, J., and Lv, J. Y.: Atmospheric isoprene and monoterpenes in a typical urban area of Beijing: Pollution
425 characterization, chemical reactivity and source identification, *J. Environ. Sci.*, doi:10.1016/j.jes.2017.12.017, 2018.
- Cheng, Y., He, K. B., Duan, F. K., Zheng, M., Du, Z. Y., Ma, Y. L., and Tan, J. H.: Ambient organic carbon to elemental
carbon ratios: Influences of the measurement methods and implications, *Atmos. Environ.*, 45, 2060-2066,
doi:10.1016/j.atmosenv.2011.01.064, 2011.
- Cheng, Y., Engling, G., He, K. B., Duan, F. K., Ma, Y. L., Du, Z. Y., Liu, J. M., Zheng, M., and Weber, R. J.: Biomass
430 burning contribution to Beijing aerosol, *Atmos. Chem. Phys.*, 13, 7765-7781, doi:10.5194/acp-13-7765-2013, 2013b.
- Cheng, Y., He, K. B., Du, Z. Y., Zheng, M., Duan, F. K., and Ma, Y. L.: Humidity plays an important role in the PM_{2.5}
pollution in Beijing, *Environ. Pollut.*, 197, 68-75, doi:10.1016/j.envpol.2014.11.028, 2015.
- Cheng, Y. F., Zheng, G. J., Wei, C., Mu, Q., Zheng, B., Wang, Z. B., Gao, M., Zhang, Q., He, K. B., Carmichael, G., Poschl,
U., and Su, H.: Reactive nitrogen chemistry in aerosol water as a source of sulfate during haze events in China, *Sci. Adv.*, 2,
435 e1601530, doi:10.1126/sciadv.1601530, 2016.



- Claeys, M., Graham, B., Vas, G., Wang, W., Vermeylen, R., Pashynska, V., Cafmeyer, J., Guyon, P., Andreae, M. O., Artaxo, P., and Maenhaut, W.: Formation of secondary organic aerosols through photooxidation of isoprene, *Science*, 303, 1173-1176, doi:10.1126/science.1092805, 2004a.
- Claeys, M., Wang, W., Ion, A. C., Kourtchev, I., Gelencser, A., and Maenhaut, W.: Formation of secondary organic aerosols from isoprene and its gas-phase oxidation products through reaction with hydrogen peroxide, *Atmos. Environ.*, 38, 4093-4098, doi:10.1016/j.atmosenv.2004.06.001, 2004b.
- Ding, X., Zheng, M., Edgerton, E. S., Jansen, J. J., and Wang, X. M.: Contemporary or fossil origin: split of estimated secondary organic carbon in the southeastern United States, *Environ. Sci. Technol.*, 42, 9122-9128, 2008a.
- Ding, X., Zheng, M., Yu, L., Zhang, X., Weber, R. J., Yan, B., Russell, A. G., Edgerton, E. S., and Wang, X. M.: Spatial and seasonal trends in biogenic secondary organic aerosol tracers and water-soluble organic carbon in the southeastern United States, *Environ. Sci. Technol.*, 42, 5171-5176, 2008b.
- Ding, X., Wang, X. M., and Zheng, M.: The influence of temperature and aerosol acidity on biogenic secondary organic aerosol tracers: Observations at a rural site in the central Pearl River Delta region, South China, *Atmos. Environ.*, 45, 1303-1311, doi:10.1016/j.atmosenv.2010.11.057, 2011.
- Du, Z. Y., He, K. B., Cheng, Y., Duan, F. K., Ma, Y. L., Liu, J. M., Zhang, X. L., Zheng, M., and Weber, R.: A yearlong study of water-soluble organic carbon in Beijing I: Sources and its primary vs. secondary nature, *Atmos. Environ.*, 92, 514-521, doi:10.1016/j.atmosenv.2014.04.060, 2014.
- Ervens, B., Turpin, B. J., and Weber, R. J.: Secondary organic aerosol formation in cloud droplets and aqueous particles (aqSOA): a review of laboratory, field and model studies, *Atmos. Chem. Phys.*, 11, 11069-11102, doi:10.5194/acp-11-11069-2011, 2011.
- Favez, O., Sciare, J., Cachier, H., Alfaro, S. C., and Abdelwahab, M. M.: Significant formation of water-insoluble secondary organic aerosols in semi-arid urban environment, *Geophys. Res. Lett.*, 35, L15801, doi:10.1029/2008GL034446, 2008.
- Feng, J. L., Li, M., Zhang, P., Gong, S. Y., Zhong, M., Wu, M. H., Zheng, M., Chen, C. H., Wang, H. L., and Lou, S. R.: Investigation of the sources and seasonal variations of secondary organic aerosols in PM_{2.5} in Shanghai with organic tracers, *Atmos. Environ.*, 79, 614-622, doi:10.1016/j.atmosenv.2013.07.022, 2013.
- Fountoukis, C. and Nenes, A.: ISORROPIA II: a computationally efficient thermodynamic equilibrium model for K⁺-Ca²⁺-Mg²⁺-NH₄⁺-Na⁺-SO₄²⁻-NO₃⁻-Cl⁻-H₂O aerosols, *Atmos. Chem. Phys.*, 7, 4639-4659, 2007.
- Fu, P. Q., Kawamura, K., Kanaya, Y., and Wang, Z. F.: Contributions of biogenic volatile organic compounds to the formation of secondary organic aerosols over Mt Tai, Central East China, *Atmos. Environ.*, 44, 4817-4826, doi:10.1016/j.atmosenv.2010.08.040, 2010.
- Gao, J. J., Tian, H. Z., Cheng, K., Lu, L., Wang, Y. X., Wu, Y. X., Zhu, C. Y., Liu, K. Y., Zhou, J. R., Liu, X. G., Chen, J., and Hao, J. M.: Seasonal and spatial variation of trace elements in multi-size airborne particulate matters of Beijing, China: Mass concentration, enrichment characteristics, source apportionment, chemical speciation and bioavailability, *Atmos. Environ.*, 99, 257-265, doi:10.1016/j.atmosenv.2014.08.081, 2014.



- 470 Guo, H. T., Zhou, J. B., Wang, L., Zhou, Y., Yuan, J. P., and Zhao, R. S.: Seasonal Variations and Sources of Carboxylic Acids in PM_{2.5} in Wuhan, China, *Aerosol Air Qual. Res.*, 15, 517-528, doi:10.4209/aaqr.2014.02.0040, 2015.
- He, L. Y., Hu, M., Huang, X. F., Zhang, Y. H., and Tang, X. Y.: Seasonal pollution characteristics of organic compounds in atmospheric fine particles in Beijing, *Sci. Total Environ.*, 359, 167-176, doi:10.1016/j.scitotenv.2005.05.044, 2006.
- Hennigan, C. J., Bergin, M. H., Russell, A. G., Nenes, A., and Weber, R. J.: Gas/particle partitioning of water-soluble
475 organic aerosol in Atlanta, *Atmos. Chem. Phys.*, 9, 3613-3628, doi:10.5194/acp-9-3613-2009, 2009.
- Herckes, P., Engling, G., Kreidenweis, S. M., and Collett, J. L., Jr.: Particle size distributions of organic aerosol constituents during the 2002 Yosemite Aerosol Characterization Study, *Environ. Sci. Technol.*, 40, 4554-4562, 2006.
- Hoyle, C. R., Boy, M., Donahue, N. M., Fry, J. L., Glasius, M., Guenther, A., Hallar, A. G., Hartz, K. H., Petters, M. D.,
Petaja, T., Rosenoern, T., and Sullivan, A. P.: A review of the anthropogenic influence on biogenic secondary organic
480 aerosol, *Atmos. Chem. Phys.*, 11, 321-343, doi:10.5194/acp-11-321-2011, 2011.
- Iinuma, Y., Boge, O., Grafe, R., and Herrmann, H.: Methyl-nitrocatechols: atmospheric tracer compounds for biomass burning secondary organic aerosols, *Environ. Sci. Technol.*, 44, 8453-8459, doi:10.1021/es102938a, 2010.
- Jaffrezo, J. L., Aymoz, G., Delaval, C., and Cozic, J.: Seasonal variations of the water soluble organic carbon mass fraction of aerosol in two valleys of the French Alps, *Atmos. Chem. Phys.*, 5, 2809-2821, doi:10.5194/acp-5-2809-2005, 2005.
- 485 Kaul, D. S., Gupta, T., and Tripathi, S. N.: Source Apportionment for Water Soluble Organic Matter of Submicron Aerosol: A Comparison between Foggy and Nonfoggy Episodes, *Aerosol Air Qual. Res.*, 14, 1527-1533, doi:10.4209/aaqr.2013.10.0319, 2014.
- Kavouras, I. G. and Stephanou, E. G.: Particle size distribution of organic primary and secondary aerosol constituents in urban, background marine, and forest atmosphere, *J. Geophys. Res.-Atmos.*, 107, 4069, doi:10.1029/2000JD000278, 2002.
- 490 Kawamura, K. and Kaplan, I. R.: Motor exhaust emissions as a primary source for dicarboxylic acids in Los-Angeles ambient air, *Environ. Sci. Technol.*, 21, 105-110, 1987.
- Kleindienst, T. E., Jaoui, M., Lewandowski, M., Offenberg, J. H., Lewis, C. W., Bhave, P. V., and Edney, E. O.: Estimates of the contributions of biogenic and anthropogenic hydrocarbons to secondary organic aerosol at a southeastern US location, *Atmos. Environ.*, 41, 8288-8300, doi:10.1016/j.atmosenv.2007.06.045, 2007.
- 495 Kuang, B. Y., Lin, P., Huang, X. H. H., and Yu, J. Z.: Sources of humic-like substances in the Pearl River Delta, China: positive matrix factorization analysis of PM_{2.5} major components and source markers, *Atmos. Chem. Phys.*, 15, 1995-2008, doi:10.5194/acp-15-1995-2015, 2015.
- Li, J. J., Wang, G. H., Wu, C., Cao, C., Ren, Y. Q., Wang, J. Y., Li, J., Cao, J. J., Zeng, L. M., and Zhu, T.: Characterization of isoprene-derived secondary organic aerosols at a rural site in North China Plain with implications for anthropogenic
500 pollution effects, *Sci. Rep.-UK*, 8, 535, doi:10.1038/s41598-017-18983-7, 2018.
- Liang, L. L., Engling, G., Duan, F. K., Cheng, Y., and He, K. B.: Characteristics of 2-methyltetrols in ambient aerosol in Beijing, China, *Atmos. Environ.*, 59, 376-381, doi:10.1016/j.atmosenv.2012.05.052, 2012.



- Lim, H. J. and Turpin, B. J.: Origins of primary and secondary organic aerosol in Atlanta: results of time-resolved measurements during the Atlanta Supersite Experiment, *Environ. Sci. Technol.*, 36, 4489-4496, 2002.
- 505 Qiao, T., Zhao, M. F., Xiu, G. L., and Yu, J. Z.: Simultaneous monitoring and compositions analysis of PM₁ and PM_{2.5} in Shanghai: Implications for characterization of haze pollution and source apportionment, *Sci. Total Environ.*, 557-558, 386-394, doi:10.1016/j.scitotenv.2016.03.095, 2016.
- Ram, K., Sarin, M. M., and Tripathi, S. N.: Temporal trends in atmospheric PM_{2.5}, PM₁₀, elemental carbon, organic carbon, water-soluble organic carbon, and optical properties: impact of biomass burning emissions in the Indo-Gangetic Plain, *Environ. Sci. Technol.*, 46, 686-695, doi:10.1021/es202857w, 2012.
- 510 Riva, M., Bell, D. M., Hansen, A. M. K., Drozd, G. T., Zhang, Z. F., Gold, A., Imre, D., Surratt, J. D., Glasius, M., and Zelenyuk, A.: Effect of organic coatings, humidity and aerosol acidity on multiphase chemistry of isoprene epoxydiols, *Environ. Sci. Technol.*, 50, 5580-5588, doi:10.1021/acs.est.5b06050, 2016.
- Sciare, J., d'Argouges, O., Sarda-Estève, R., Gaimoz, C., Dolgorouky, C., Bonnaire, N., Favez, O., Bonsang, B., and Gros, V.: Large contribution of water-insoluble secondary organic aerosols in the region of Paris (France) during wintertime, *J. Geophys. Res.-Atmos.*, 116, D22203, doi:10.1029/2011JD015756, 2011.
- 515 Shen, R. Q., Ding, X., He, Q. F., Cong, Z. Y., Yu, Q. Q., and Wang, X. M.: Seasonal variation of secondary organic aerosol tracers in Central Tibetan Plateau, *Atmos. Chem. Phys.*, 15, 8781-8793, doi:10.5194/acp-15-8781-2015, 2015.
- Surratt, J. D., Chan, A. W., Eddingsaas, N. C., Chan, M., Loza, C. L., Kwan, A. J., Hersey, S. P., Flagan, R. C., Wennberg, P. O., and Seinfeld, J. H.: Reactive intermediates revealed in secondary organic aerosol formation from isoprene, *P. Natl. Sci. USA*, 107, 6640-6645, doi:10.1073/pnas.0911114107, 2010.
- 520 Tang, X., Zhang, X. S., Wang, Z. W., and Ci, Z. J.: Water-soluble organic carbon (WSOC) and its temperature-resolved carbon fractions in atmospheric aerosols in Beijing, *Atmospheric Research*, 181, 200-210, doi:10.1016/j.atmosres.2016.06.019, 2016.
- 525 Tao, J., Zhang, L. M., Zhang, R. J., Wu, Y. F., Zhang, Z. S., Zhang, X. L., Tang, Y. X., Cao, J. J., and Zhang, Y. H.: Uncertainty assessment of source attribution of PM_{2.5} and its water-soluble organic carbon content using different biomass burning tracers in positive matrix factorization analysis—a case study in Beijing, China, *Sci. Total Environ.*, 543, 326-335, doi:10.1016/j.scitotenv.2015.11.057, 2016.
- Tian, S. L., Pan, Y. P., Liu, Z. R., Wen, T. X., and Wang, Y. S.: Size-resolved aerosol chemical analysis of extreme haze pollution events during early 2013 in urban Beijing, China, *J. Hazard. Mater.*, 279, 452-460, doi:10.1016/j.jhazmat.2014.07.023, 2014.
- 530 Velali, E., Papachristou, E., Pantazaki, A., Choli-Papadopoulou, T., Planou, S., Kouras, A., Manoli, E., Besis, A., Voutsas, D., and Samara, C.: Redox activity and in vitro bioactivity of the water-soluble fraction of urban particulate matter in relation to particle size and chemical composition, *Environ. Pollut.*, 208, 774-786, doi:10.1016/j.envpol.2015.10.058, 2016.



- 535 Xiang, P., Zhou, X. M., Duan, J. C., Tan, J. H., He, K. B., Yuan, C., Ma, Y. L., and Zhang, Y. X.: Chemical characteristics of water-soluble organic compounds (WSOC) in PM_{2.5} in Beijing, China: 2011–2012, *Atmospheric Research*, 183, 104–112, doi:10.1016/j.atmosres.2016.08.020, 2017.
- Xu, L., Guo, H. Y., Boyd, C. M., Klein, M., Bougiatioti, A., Cerully, K. M., Hite, J. R., Isaacman-VanWertz, G., Kreisberg, N. M., Knote, C., Olson, K., Koss, A., Goldstein, A. H., Hering, S. V., de Gouw, J., Baumann, K., Lee, S. H., Nenes, A.,
- 540 Weber, R. J., and Ng, N. L.: Effects of anthropogenic emissions on aerosol formation from isoprene and monoterpenes in the southeastern United States, *P. Natl. Sci. USA*, 112, 37–42, doi:10.1073/pnas.1417609112, 2015.
- Yan, C. Q., Zheng, M., Sullivan, A. P., Bosch, C., Desyaterik, Y., Andersson, A., Li, X. Y., Guo, X. S., Zhou, T., Gustafsson, O., and Collett, J. L.: Chemical characteristics and light-absorbing property of water-soluble organic carbon in Beijing: Biomass burning contributions, *Atmos. Environ.*, 121, 4–12, doi:10.1016/j.atmosenv.2015.05.005, 2015.
- 545 Yang, F., Kawamura, K., Chen, J., Ho, K., Lee, S., Gao, Y., Cui, L., Wang, T. G., and Fu, P. Q.: Anthropogenic and biogenic organic compounds in summertime fine aerosols PM_{2.5} in Beijing, China, *Atmos. Environ.*, 124, 166–175, doi:10.1016/j.atmosenv.2015.08.095, 2016a.
- Yang, H. N., Chen, J., Wen, J. J., Tian, H. Z., and Liu, X. G.: Composition and sources of PM_{2.5} around the heating periods of 2013 and 2014 in Beijing: Implications for efficient mitigation measures, *Atmos. Environ.*, 124, 378–386,
- 550 doi:10.1016/j.atmosenv.2015.05.015, 2016b.
- Yu, J. Z., Cocker, D. R., Griffin, R. J., Flagan, R. C., and Seinfeld, J. H.: Gas-phase ozone oxidation of monoterpenes: Gaseous and particulate products, *J Atmos Chem*, 34, 207–258, 1999.
- Zhang, Y. P., Chen, J., Yang, H. N., Li, R. J., and Yu, Q.: Seasonal variation and potential source regions of PM_{2.5}-bound PAHs in the megacity Beijing, China: Impact of regional transport, *Environ. Pollut.*, 231, 329–338,
- 555 doi:10.1016/j.envpol.2017.08.025, 2017.
- Zhao, W. Y., Kawamura, K., Yue, S. Y., Wei, L. F., Ren, H., Yan, Y., Kang, M. J., Li, L. J., Ren, L. J., Lai, S. C., Li, J., Sun, Y. L., Wang, Z. F., and Fu, P. Q.: Molecular distribution and compound-specific stable carbon isotopic composition of dicarboxylic acids, oxocarboxylic acids and α -dicarbonyls in PM_{2.5} from Beijing, China, *Atmos. Chem. Phys.*, 18, 2749–2767, doi:10.5194/acp-18-2749-2018, 2018.
- 560 Zheng, M., Ke, L., Edgerton, E. S., Schauer, J. J., Dong, M. Y., and Russell, A. G.: Spatial distribution of carbonaceous aerosol in the southeastern United States using molecular markers and carbon isotope data, *J. Geophys. Res.-Atmos.*, 111, D10S06, doi:10.1029/2005JD006777, 2006.
- Zhou, S. Z., Wang, T., Wang, Z., Li, W. J., Xu, Z., Wang, X. F., Yuan, C., Poon, C. N., Louie, P. K. K., Luk, C. W. Y., and Wang, W. X.: Photochemical evolution of organic aerosols observed in urban plumes from Hong Kong and the Pearl River
- 565 Delta of China, *Atmos. Environ.*, 88, 219–229, doi:10.1016/j.atmosenv.2014.01.032, 2014.
- Zhou, Y., Zhang, H. F., Parikh, H. M., Chen, E. H., Rattanavaraha, W., Rosen, E. P., Wang, W. X., and Kamens, R. M.: Secondary organic aerosol formation from xylenes and mixtures of toluene and xylenes in an atmospheric urban



hydrocarbon mixture: Water and particle seed effects (II), Atmos. Environ., 45, 3882-3890,
doi:10.1016/j.atmosenv.2010.12.048, 2011.



571

Table 1. Average concentrations of the identified species in PM₁, PM_{2.5} and PM₁₀ during haze episodes (PM_{2.5}>75 µg m⁻³) in winter and spring.

Compounds	Winter									Spring								
	PM ₁			PM _{2.5}			PM ₁₀			PM ₁			PM _{2.5}			PM ₁₀		
	Day	Night	Total	Day	Night	Total	Day	Night	Total	Day	Night	Total	Day	Night	Total	Day	Night	Total
WSOC (µg m ⁻³)	14.1	15.3	14.7	27.0	31.1	29.2	31.7	34.8	33.4	6.6	6.0	6.3	9.2	8.8	9.0	11.4	10.5	10.9
OC (µg m ⁻³)	22.1	24.4	23.4	40.4	47.4	44.1	48.3	55.4	52.1	9.1	8.8	9.0	12.7	12.8	12.8	16.6	16.6	16.6
EC (µg m ⁻³)	5.5	7.9	6.8	9.0	12.2	10.7	10.5	13.4	12.1	2.3	2.6	2.4	3.5	4.2	3.8	4.6	5.1	4.9
WSOC/OC	0.66	0.60	0.63	0.67	0.64	0.65	0.65	0.61	0.63	0.77	0.73	0.75	0.74	0.70	0.72	0.70	0.69	0.69
OC/EC	4.01	3.38	3.68	4.40	4.07	4.22	4.47	4.16	4.30	4.08	3.62	3.84	3.73	3.17	3.44	3.77	3.33	3.54
Particulate matter (µg m ⁻³)	157.1	168.6	163.2	277.6	306.6	293.1	348.6	379.4	365.0	111.6	105.9	108.6	152.6	152.3	152.4	215.2	217.7	216.5
Organic tracers (ng m⁻³)																		
Levoglucosan	427.6	546.1	490.8	693.7	977.5	845.0	805.2	1123.2	974.8	151.1	210.1	182.9	265.2	443.0	361.0	361.2	560.8	468.6
Cholesterol	16.2	19.0	17.7	18.5	31.8	25.6	22.5	37.9	30.7	8.1	7.2	7.7	9.6	10.2	9.9	12.8	14.1	13.5
4-Methyl-5-nitrocatechol	107.5	119.4	113.8	163.5	227.4	197.6	187.6	288.2	241.2	23.8	22.0	22.8	34.1	46.9	41.0	37.0	54.2	46.3
Phthalic acid	81.9	82.3	82.1	187.1	233.1	211.6	233.8	294.9	266.4	25.1	22.9	23.8	36.0	38.5	37.4	48.3	45.0	46.4
2-Methylerythritol	3.9	3.9	3.9	7.1	8.0	7.6	10.5	11.8	11.2	2.5	2.6	2.6	3.4	4.3	3.9	4.3	6.3	5.3
3-Hydroxyglutaric acid	3.7	3.1	3.4	8.6	8.8	8.7	10.4	10.8	10.6	5.5	5.1	5.3	10.2	11.6	11.0	12.7	12.8	12.8
<i>Cis</i> -pinonic acid	2.7	1.6	2.1	3.1	2.4	2.7	3.6	3.1	3.3	5.9	3.7	4.7	6.5	4.5	5.4	8.0	5.4	6.6
Water-soluble ions (µg m⁻³)																		
Nitrate, NO ₃ ⁻	22.85	17.75	20.13	40.49	35.89	38.04	47.72	43.74	45.60	17.90	16.28	17.06	31.72	29.42	30.52	37.57	35.24	36.36
Sulfate, SO ₄ ²⁻	13.66	13.01	13.31	30.24	33.19	31.81	36.70	41.27	39.14	6.27	5.84	6.05	11.56	11.04	11.29	13.71	13.20	13.44
Chloride, Cl ⁻	2.69	3.12	2.92	4.31	5.25	4.81	6.35	7.14	6.77	1.18	1.17	1.18	1.93	1.87	1.90	2.72	2.64	2.68
Oxalate, C ₂ O ₄ ²⁻	0.65	0.58	0.61	1.00	0.99	0.99	1.20	1.28	1.24	0.37	0.34	0.35	0.60	0.61	0.60	0.73	0.76	0.75
Ammonium, NH ₄ ⁺	12.01	10.26	11.08	21.44	22.22	21.85	24.85	26.01	25.47	7.10	6.71	6.90	11.91	11.44	11.67	13.15	12.43	12.78
Potassium, K ⁺	1.06	1.06	1.06	1.84	2.05	1.95	2.17	2.40	2.29	0.67	0.67	0.67	1.17	1.13	1.15	1.37	1.31	1.34
Calcium, Ca ²⁺	0.86	0.71	0.78	0.78	0.69	0.74	3.02	2.94	2.98	1.21	1.05	1.13	1.04	0.90	0.96	4.35	3.94	4.14
Sodium, Na ⁺	0.65	0.57	0.61	0.75	0.75	0.75	1.92	1.52	1.71	0.32	0.27	0.30	0.39	0.37	0.38	0.78	0.74	0.76
Magnesium, Mg ²⁺	0.16	0.12	0.14	0.20	0.18	0.19	0.59	0.56	0.57	0.15	0.12	0.13	0.17	0.14	0.15	0.47	0.44	0.46



Table 2. Spearman correlation coefficients between the SOA tracers and meteorological parameters, O₃, aerosol acidity (H⁺), and aerosol water content (AWC) in PM₁, PM_{2.5} and PM₁₀ during the whole sampling period ^a.

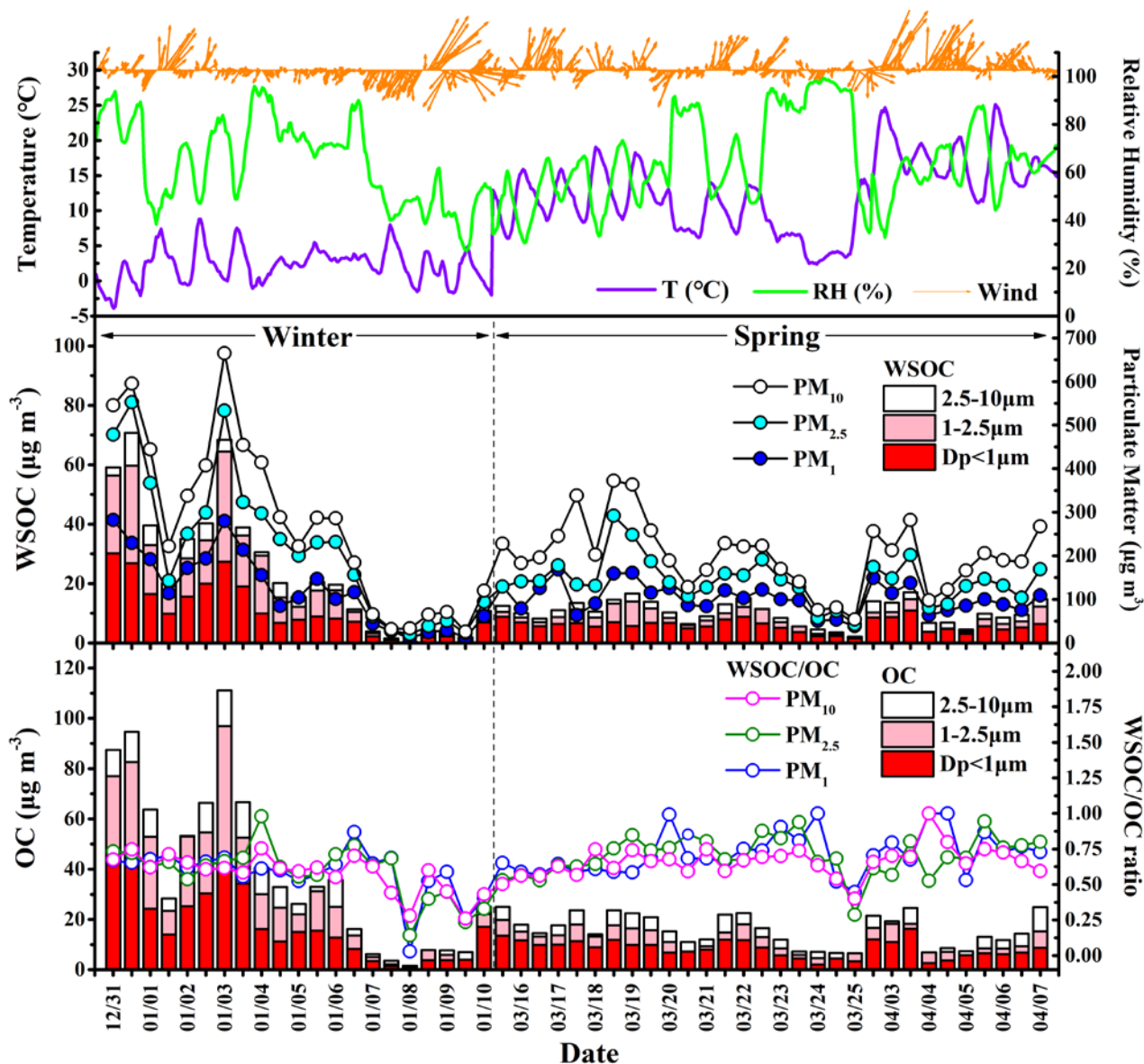
Compounds	Size	T	RH	WS	SR ^b	O ₃	H ⁺ ^c	AWC
4-Methyl-5-nitrocatechol	PM ₁	-0.36*	0.50**	-0.63**	-0.52*	-0.67**	0.39**	0.65**
	PM _{2.5}	-0.34*	0.52**	-0.67**	-0.48*	-0.66**	0.36*	0.68**
	PM ₁₀	-0.33*	0.52**	-0.65**	-0.49*	-0.64**	0.25	0.70**
Phthalic acid	PM ₁	-0.50**	0.28	-0.45**	-0.64**	-0.68**	0.30	0.61**
	PM _{2.5}	-0.52**	0.39**	-0.57**	-0.64**	-0.69**	0.58**	0.70**
	PM ₁₀	-0.48**	0.41**	-0.57**	-0.65**	-0.65**	0.38*	0.73**
2-Methylerythritol	PM ₁	0.04	0.47**	-0.40**	-0.20	-0.18	0.03	0.55**
	PM _{2.5}	-0.06	0.58**	-0.47**	-0.31	-0.30*	0.36*	0.65**
	PM ₁₀	-0.11	0.63**	-0.52**	-0.45*	-0.37*	0.37*	0.68**
3-Hydroxyglutaric acid	PM ₁	0.59**	0.14	-0.16	0.27	0.37*	0.25	0.28
	PM _{2.5}	0.38*	0.42**	-0.38*	0.03	0.17	0.48**	0.51**
	PM ₁₀	0.32*	0.48**	-0.39*	-0.03	0.12	0.26	0.53**
<i>Cis</i> -pinonic acid	PM ₁	0.76**	-0.08	-0.05	0.33	0.46**	0.14	0.09
	PM _{2.5}	0.72**	-0.10	-0.02	0.42	0.48**	0.37*	0.10
	PM ₁₀	0.67**	-0.07	-0.07	0.40	0.43**	-0.15	0.13
WSOC/OC	PM ₁	0.37**	0.30*	0.09	-0.11	0.30*	-0.03	0.20
	PM _{2.5}	0.27	0.51**	-0.25	-0.07	0.10	0.39**	0.50**
	PM ₁₀	0.35*	0.28*	0.13	0.18	0.39**	0.26	0.26

^a A precipitation process occurred between the night of March 22nd and the night of March 24th, thus was excluded from the correlation analysis.

575 ^b Solar radiation at night was close to zero, thus only the daytime data were included in the correlation analysis.

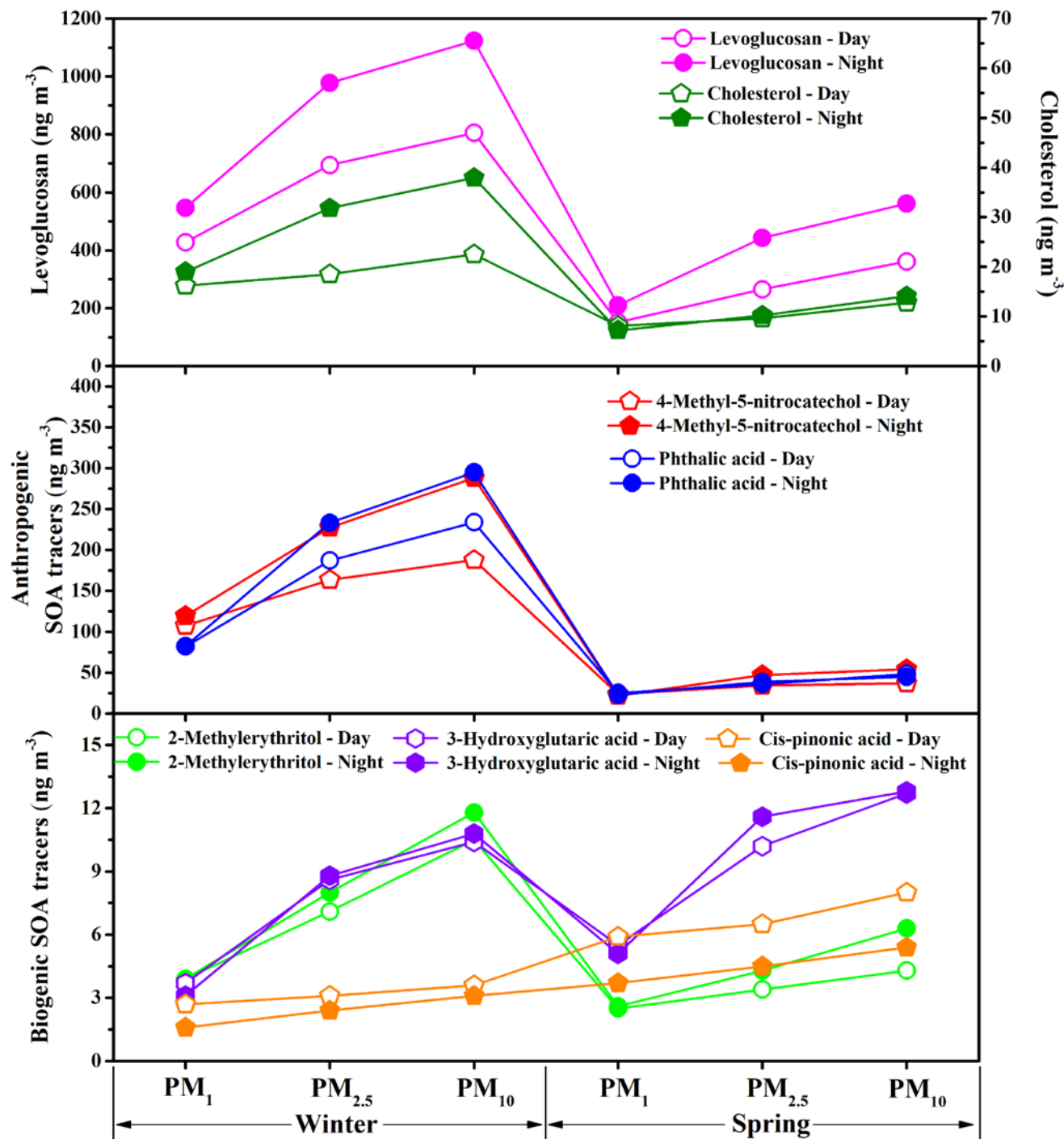
^c $[H^+] = 2[SO_4^{2-}] + [NO_3^-] + [Cl^-] + 2[C_2O_4^{2-}] - [Na^+] - [NH_4^+] - [K^+] - 2[Mg^{2+}] - 2[Ca^{2+}]$.

Level of significance: *: $p < 0.05$; **: $p < 0.01$.

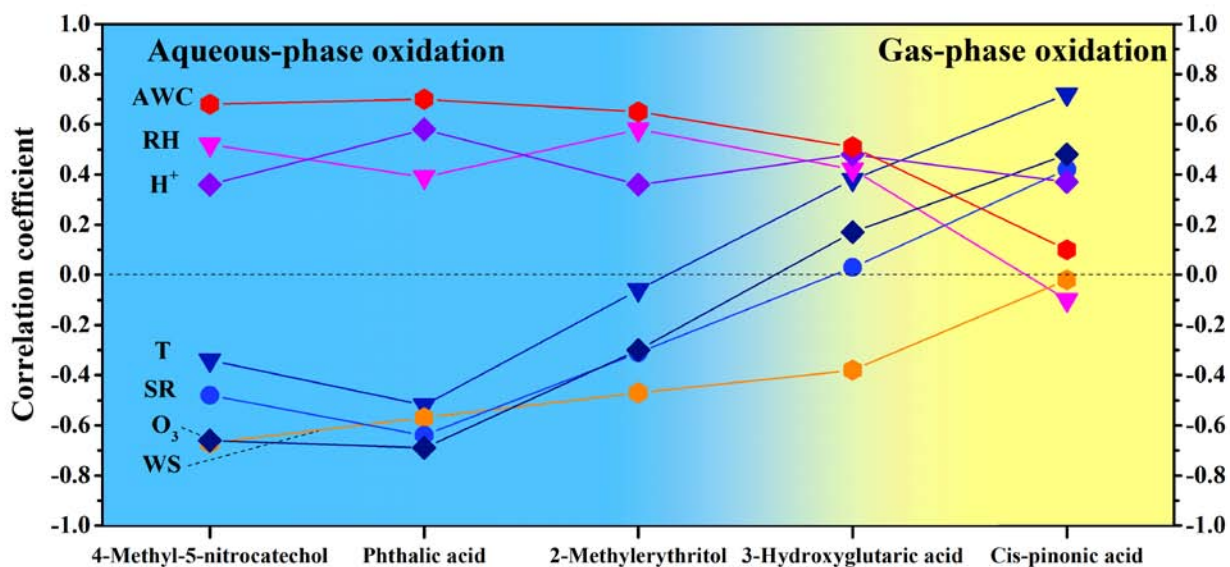


580

Figure 1. Temporal variations of meteorological conditions and WSOC, OC and particulate mass concentrations in PM_{10} , $PM_{2.5}$ and PM_1 in Beijing during the whole sampling period.



585 **Figure 2.** Diurnal variations of the average mass concentrations of organic tracers in PM_1 , $PM_{2.5}$ and PM_{10} during the haze episodes ($PM_{2.5} > 75 \mu g m^{-3}$) in winter and spring.



590 **Figure 3.** Comparison of the Spearman correlation coefficients with meteorological parameters, O₃, aerosol acidity (H⁺), and aerosol water content (AWC) in PM_{2.5} among different SOA tracers.

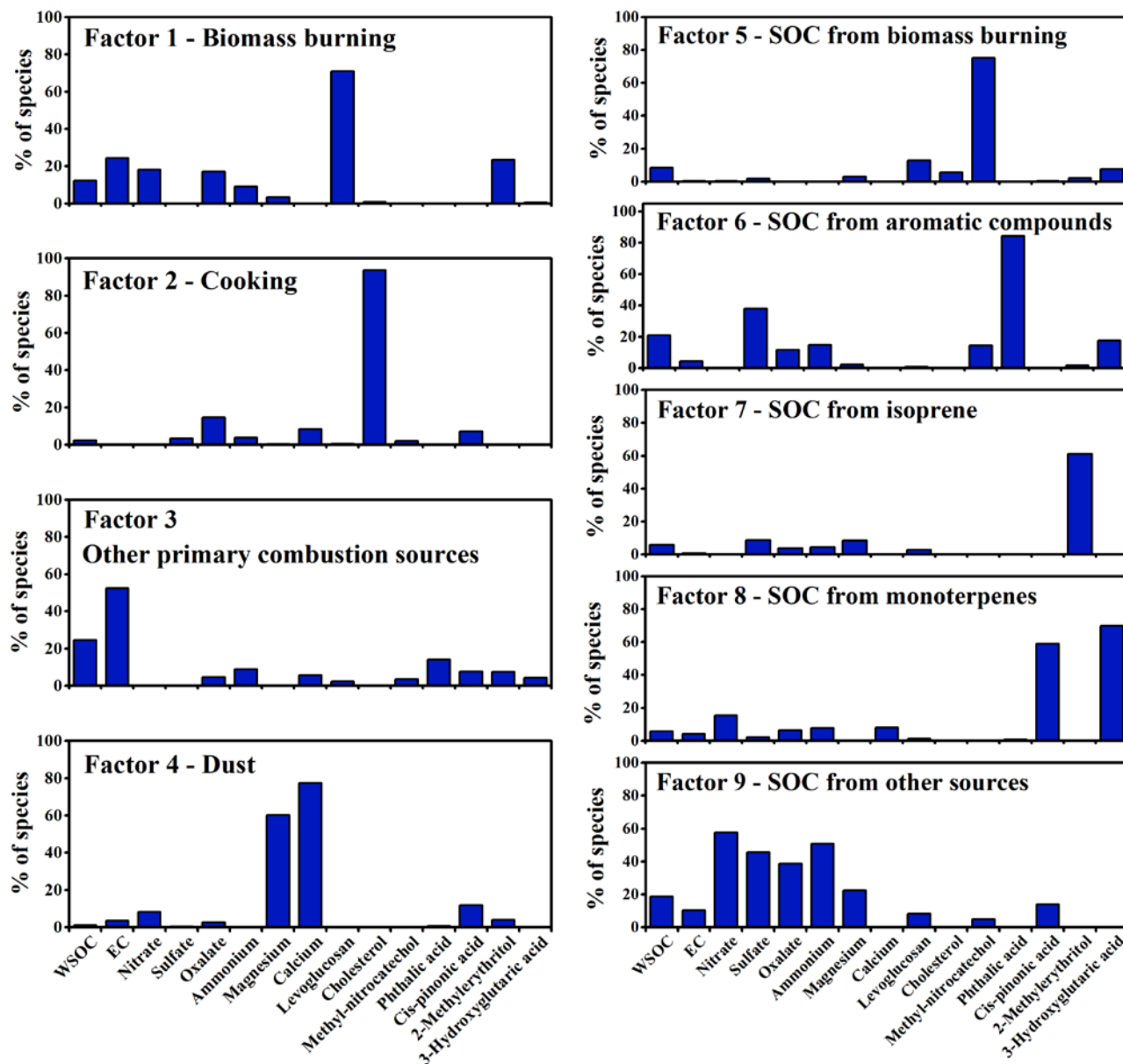


Figure 4. Source profiles of WSOC in atmospheric particulate matter in Beijing resolved by PMF.

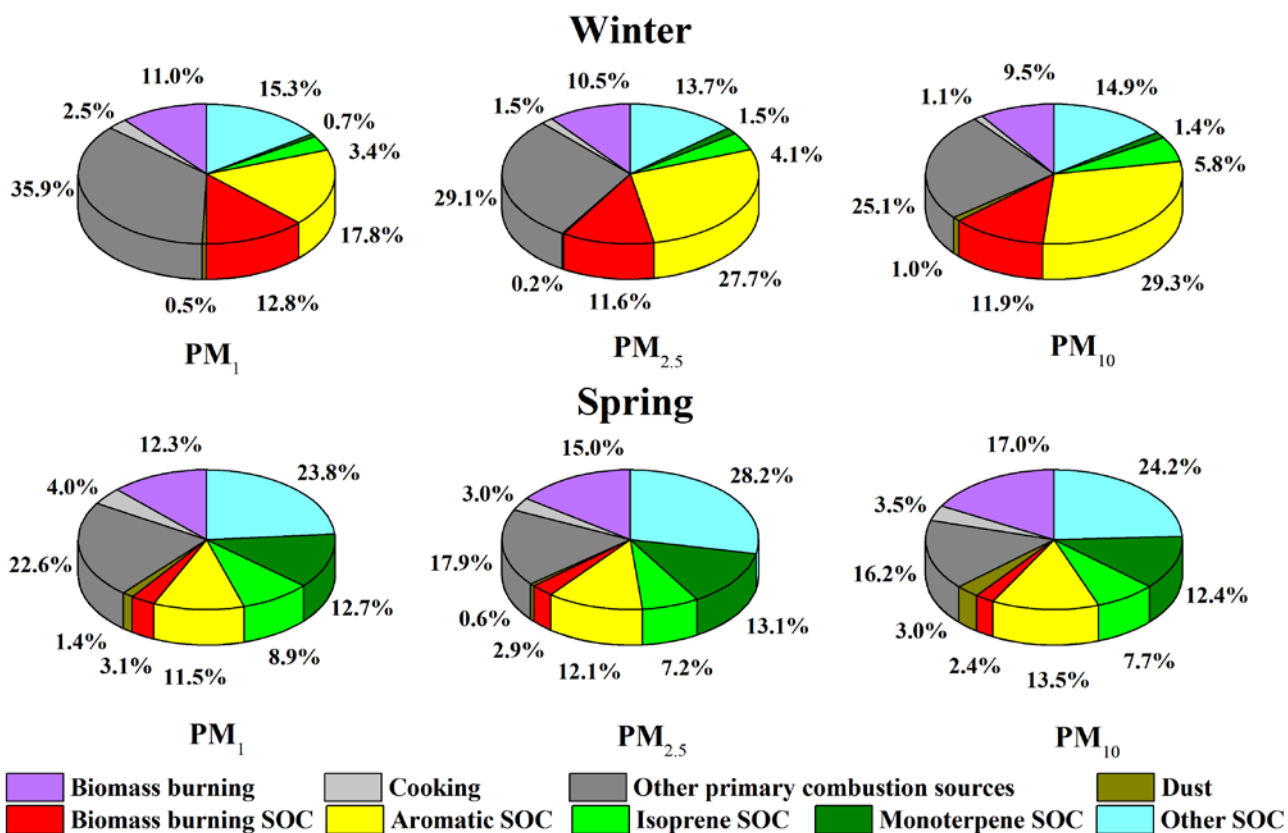


Figure 5. Source contributions to WSOC in PM₁, PM_{2.5} and PM₁₀ in Beijing during the sampling periods in winter and spring.

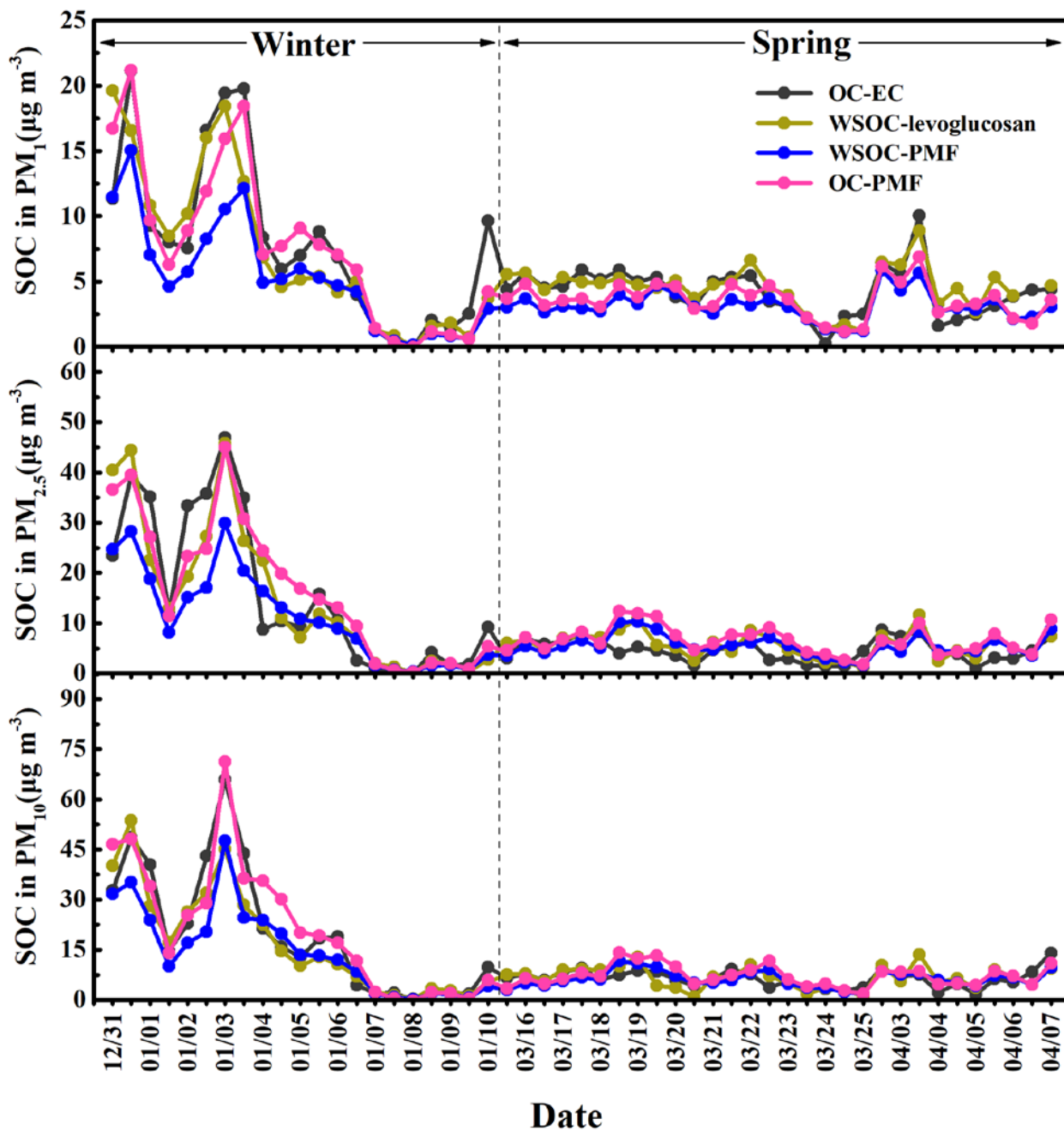


Figure 6. Comparison of secondary organic carbon in PM_1 , $PM_{2.5}$ and PM_{10} in Beijing estimated by the OC-EC method, WSOC-levoglucosan method and PMF-based methods during the sampling periods in winter and spring.